Nucl. Fusion **50** (2010) 125009 (5pp) doi:10.1088/0029-5515/50/12/125009

Forced chemical confinement fusion: μ-catalysed fusion by taking resonance escape probability of tμ(1s) atoms using an alternative kinetic model

R. Gheisari

Physics Department, Persian Gulf University, Bushehr 75169, Iran

E-mail: gheisari@pgu.ac.ir

Received 26 May 2010, accepted for publication 19 August 2010
Published 18 November 2010
Online at stacks.iop.org/NF/50/125009

Abstract
The emission of tμ atoms in a two-layer arrangement consisting of H/T and D_2 is investigated with an alternative kinetic model. The slowing down of tμ(1s) atoms in pure deuterium and their falling down into resonance regions force chemical confinement fusion (μCF). By considering the resonance escape probability of tμ(1s) atoms, point kinematic equations are numerically solved to obtain the muon conversion efficiency and also the cycling coefficient. Under the optimal condition we show that the μ-cycling coefficient and the efficiency equal 104.5 ± 2.5 and $\sim$0.7%, respectively. Our model is compared with previous suggestions. The muon conversion efficiency is estimated for a possible design and compared with recent experimental results for H/T $\oplus$ D/T.

1. Introduction

Negative muons (1–10 MeV) can stop and form muonic atoms (μt, μd and μp) in different solid hydrogen targets cooled to 3 K [1, 2]. Such atoms, created in the excited states, cascade to the ground state quickly (10^{-12} s) [1], where their energy is much higher than the thermal equilibrium energies. The scattering reactions,

$$\mathrm{p}\mu(1\mathrm{s}) + \mathrm{H}_2 \longrightarrow \mathrm{p}\mu(1\mathrm{s}) + \mathrm{H}_2, \tag{1}$$

$$\mathrm{t}\mu(1\mathrm{s}) + \mathrm{H}_2 \xrightarrow{\sigma_s^{\mathrm{el.}}(E)} \mathrm{t}\mu(1\mathrm{s}) + \mathrm{H}_2, \tag{2}$$

can take place in the H_2/T_2 targets. The solid target including a mixture of protium with a small concentration of tritium is a powerful source of energetic tμ(1s) due to the so-called Ramsauer–Townsend (RT) effect. In most cases (70–75%) the muon transfers from μp to a triton [3, 4], forming μt atoms as follows:

$$\mathrm{p}\mu(1\mathrm{s}) + \mathrm{t} \xrightarrow{\lambda_{\mathrm{pt}}(E)} \mathrm{t}\mu(1\mathrm{s}) + \mathrm{p}. \tag{3}$$

In reaction (3), the muonic tritium atom has a relatively high kinetic energy, about 45 eV. $\lambda_{\mathrm{pt}}(E)$ is the isotope exchange rate versus energy [5]. These atoms subsequently lose their energy in elastic collisions (2), until the energy reaches the range of the RT minimum in the cross section $\sigma_s^{\mathrm{el.}}(E)$. Then the mean distance between collisions increases and the H_2/T_2 layer becomes effectively transparent for the μt atoms. The use of RT minimum for the purpose of selecting muonic atoms of a certain range of low energies has long been discussed in the muon-catalysed-fusion community. The research group of [3] selected this target as an emitter of μt atoms and kept the D_2 targets frozen on it to allow muonic molecules to be formed resonantly. In principle, they proposed an arrangement which repeats formation and fusion layers periodically, as given in figure 1. They wrote point kinematics equations for their system, where a much larger value of the cycling coefficient is claimed under inaccurate assumptions. In this paper, we focus on a multilayer source of slow muon/muonic atoms to study thin materials. Our model and methodology are given in section 2. In section 3, we present and discuss our results. Conclusions, as well as the future perspectives of this study, are given in section 4.

2. Our model and resonance escape of emitted muonic atoms

According to the experiments [6, 7], the energy of a released muon from dtμ fusion is about 10 keV. The 10 keV (or below) muons have less chance to be released from the surface of the fusion layer. Such muons stop in the range of $l_\mu \approx 0.3$ μm due to high stopping power. The muon conversion efficiency from $\sim$1 MeV to 10 keV is estimated to be a little more than 0.01 in the arrangement H/T $\oplus$ D/T. RIKEN-RAL, PSI and KEK muon facilities reported that the probability of a muon entering

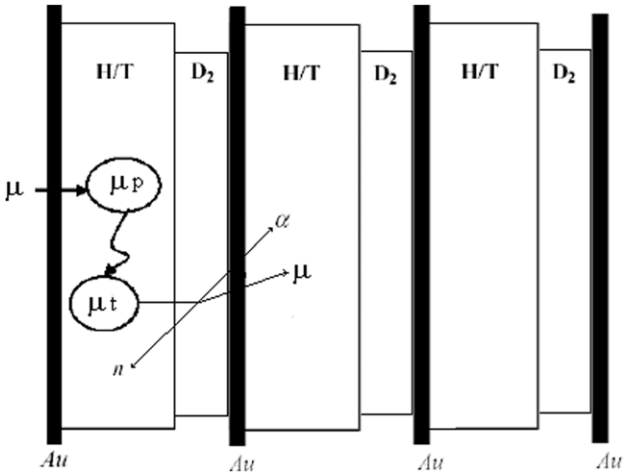

Figure 1. The suggested system of the research group of [3].

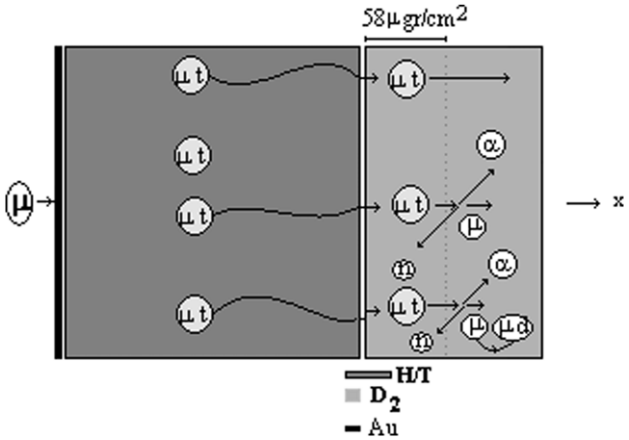

Figure 2. Diagram of the target. It includes the first layer as the production layer and the second as the fusion layer. The x-axis shows the beam axis (reactor axis). The thickness of the degrader is approximately $\simeq 58\,\mu\mathrm{g\,cm^{-2}}$.

the next layer is of the order of up to 1%, under the condition that the thickness of the fusion layer D/T becomes $\simeq 1\,\mu$m [6, 7]. However, the thickness of each fusion layer used in [3] was about 5 μm, where the efficiency of slow μ^- production is substantially smaller due to a slower molecular formation rate in D_2 and a larger muon sticking probability to ^{3}He after fusion. Here, we propose an arrangement, which includes only two layers, as given in figure 2. One of the key steps of the present system is the dtμ resonance formation,

$$\mathrm{t}\mu(1\mathrm{s}) + (\mathrm{D}_2)_{\nu_\mathrm{i},K_\mathrm{i}} \xrightarrow{\lambda^{\mathrm{res.}}_{\mathrm{dt}\mu}(E_r)} [(\mathrm{dt}\mu)^*_{J\nu=11}\mathrm{dee}]^*_{\nu_\mathrm{f},K_\mathrm{f}}. \qquad (4)$$

$(\nu_\mathrm{i}, K_\mathrm{i})$ and $(\nu_\mathrm{f}, K_\mathrm{f})$ are the vibrational–rotational quantum numbers of the deuterium molecule and the molecular complex, respectively. E_r $(r = 1, 2, 3)$ is the energy of the resonance peak, where $E_1 = 1.5$, $E_2 = 1$ or $E_3 \simeq 0.5$ eV. The dtμ molecular ion is formed in a loosely bound state $(J = 1, \nu = 1)$ [8]. The high yield of muon catalysed fusion μCF was predicted theoretically [9, 10] on the basis of the Vesman mechanism of dtμ resonance formation [10] and was confirmed experimentally [11]. The first layer with an impurity $c_\mathrm{t} \sim 10^{-3}$ and a thickness of $\sim$1 mm efficiently

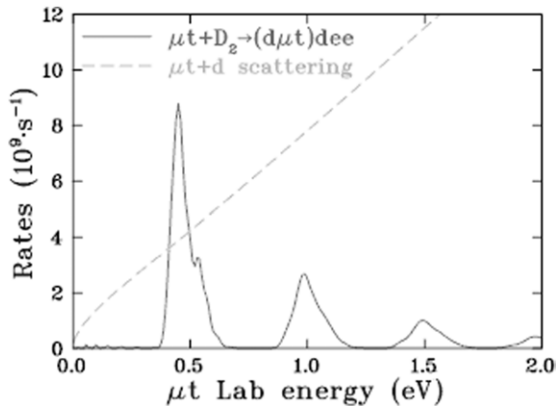

Figure 3. The resonance formation [13, 14] and elastic scattering rates [15]. Emitted μt atoms may match the resonance energy intervals.

converts the stopped muons into a μt atom beam, where large fractions of the muons transfer from μp atoms to triton nuclei. The emitted atoms can significantly form muonic molecules via reaction (4). Before resonance reactions take place, the emitted atoms are degraded using an amount of deuterium ($\simeq 58\,\mu\mathrm{g\,cm^{-2}}$). This amount of material is a part of a layer of the whole D_2 layer, as shown in figure 2. We define $N^{\mathrm{Con.}}_{\mu\mathrm{t}}(t)$ to be the population of μt atoms emitted from the surface of a degrader. The mean energy of the degraded atoms equals $\bar{E}_0 = 2.2$ eV [12]. These atoms fall down to reach the resonance regions of figure 3 [13–15]. Since the tμ(1s) atoms are neutral and very small, they lose their energy and fall down similar to neutrons [16]. The probability of falling down into the resonance energy interval δE_r is calculated by the fraction $\delta E_r/\bar{E}_0(1-\alpha)$, where δE_r approximately equals $\approx$0.337–0.382 eV. α denotes the collision parameter in the scattering of μt atoms and equals $((m_{\mu\mathrm{t}} - m_\mathrm{d})/(m_{\mu\mathrm{t}} + m_\mathrm{d}))^2$. The parameter α means the ratio of the minimum energy to the initial energy of tμ(1s) during collision. The point kinematic equations for the two-layer arrangement are introduced as follows. The equation set,

$$\frac{\mathrm{d}N^0_\mu(t)}{\mathrm{d}t} = -(\lambda_0 + \lambda_\mathrm{a}\phi_0)N^0_\mu(t), \qquad (5)$$

$$\frac{\mathrm{d}N^0_{\mu\mathrm{t}_{1\mathrm{s}}}(t)}{\mathrm{d}t} = 0.25\phi_0 c_\mathrm{t}\lambda_{\mathrm{pt}}N_{\mu\mathrm{p}_{1\mathrm{s}}}(t) - \lambda_0 N^0_{\mu\mathrm{t}_{1\mathrm{s}}}(t) + \phi_0 c_\mathrm{t}\lambda_\mathrm{a}N^0_\mu - \phi_0 c_\mathrm{p}\lambda_{\mathrm{pt}\mu}N^0_{\mu\mathrm{t}_{1\mathrm{s}}}(t) - \phi_0 c_\mathrm{t}\lambda_{\mathrm{tt}\mu}N^0_{\mu\mathrm{t}_{1\mathrm{s}}}(t), \qquad (6)$$

$$\frac{\mathrm{d}N_{\mu\mathrm{p}_{1\mathrm{s}}}(t)}{\mathrm{d}t} = -\lambda_0 N_{\mu\mathrm{p}_{1\mathrm{s}}}(t) - \phi_0 c_\mathrm{t}\lambda_{\mathrm{pt}}N_{\mu\mathrm{p}_{1\mathrm{s}}}(t) + \phi_0 c_\mathrm{p}\lambda_\mathrm{a}N^0_\mu(t) - \phi_0 c_\mathrm{p}\lambda_{\mathrm{pp}\mu}N_{\mu\mathrm{p}_{1\mathrm{s}}}(t), \qquad (7)$$

$$\frac{\mathrm{d}N_{\mathrm{pt}\mu}(t)}{\mathrm{d}t} = \phi_0 c_\mathrm{p}\lambda_{\mathrm{pt}\mu}N^0_{\mu\mathrm{t}_{1\mathrm{s}}}(t) - (\lambda^\mathrm{f}_{\mathrm{pt}\mu} + \lambda_0)N_{\mathrm{pt}\mu}(t), \qquad (8)$$

$$\frac{\mathrm{d}N_{\mathrm{tt}\mu}(t)}{\mathrm{d}t} = \phi_0 c_\mathrm{t}\lambda_{\mathrm{tt}\mu}N^0_{\mu\mathrm{t}_{1\mathrm{s}}}(t) - (\lambda^\mathrm{f}_{\mathrm{tt}\mu} + \lambda_0)N_{\mathrm{tt}\mu}(t), \qquad (9)$$

is for the first layer and the set,

$$\frac{\mathrm{d}N_\mu(t)}{\mathrm{d}t} = -(\lambda_0 + \lambda_\mathrm{a}\phi)N_\mu(t) + \lambda^\mathrm{f}_{\mathrm{dt}\mu}N_{\mathrm{dt}\mu}(t)(1 - \omega^{\mathrm{eff.}}_\mathrm{s}) + \lambda^\mathrm{f}_{\mathrm{dd}\mu}N_{\mathrm{dd}\mu}(1 - 0.58\omega_{\mathrm{dd}}), \qquad (10)$$

Table 1. The used rates (s^{-1}) and other design parameters of the two-layer arrangement.

λ_0	Muonic decay rate	0.455×10^6	[22]
λ_a	Muonic atom formation rate	$(3.9–4) \times 10^{12}$	[5, 23]
$\lambda_{tt\mu}$	$tt\mu$ formation rate	1.8×10^6	[1]
$\lambda_{pt\mu}$	$pt\mu$ formation rate	7.5×10^6	[24]
$\lambda_{pp\mu}$	$pp\mu$ formation rate	3.21×10^6	[25]
$\tilde{\lambda}^{3/2}_{dd\mu}$	$dd\mu^{3/2}$ formation rate	2.71×10^6	[18]
$\tilde{\lambda}^{1/2}_{dd\mu}$	$dd\mu^{1/2}$ formation rate	0.044×10^6	[18]
$\tilde{\lambda}^{3/2\ 1/2}_{d\mu}$	Spin flip rate	34.2×10^6	[18]
λ_{pt}	Isotope exchange rate	0.93×10^{10}	[5]
$\lambda_{dt\mu}$	Non-resonant formation rate of $dt\mu$	3×10^8	[23]
$f^{non.}$	Fractions of μt that do not make the resonance	$\simeq 0.55 \pm 0.03$	This work
$\lambda^{res.}_{dt\mu}(0.5\,eV)$	Formation rate of $dt\mu$ in $E \simeq 0.5\,eV$	$\simeq (0.81–0.89) \times 10^{10}$	[13, 14]
$\lambda^{res.}_{dt\mu}(1\,eV)$	Formation rate of $dt\mu$ in $E = 1\,eV$	$\simeq 0.27 \times 10^{10}$	[13, 14]
$\lambda^{res.}_{dt\mu}(1.5\,eV)$	Formation rate of $dt\mu$ in $E = 1.5\,eV$	$\simeq 0.146 \times 10^{10}$	[13, 14]
$\lambda^{f}_{tt\mu}$	Fusion rate for $tt\mu$	1.5×10^7	[26]
$\lambda^{f}_{pt\mu}$	Fusion rate for $pt\mu$	7×10^4	[27]
$\lambda^{f}_{dd\mu}$	Fusion rate for $dd\mu$	0.31×10^9	[22]
$\lambda^{f}_{dt\mu}$	Fusion rate for $dt\mu$	1.1×10^{12}	[5]
$\omega^{eff.}_s$	Muon sticking in $dt\mu$ branch	$\simeq 0.005$	[19]
ω_{dd}	Muon sticking in $dd\mu$ branch	$\simeq 0.122$	[18]

$$\frac{dN_{dd\mu}(t)}{dt} = \phi(\tilde{\lambda}^{3/2}_{dd\mu}N^{3/2}_{\mu d_{1s}}(t) + \tilde{\lambda}^{1/2}_{dd\mu}N^{1/2}_{\mu d_{1s}}(t)) - (\lambda^{f}_{dd\mu} + \lambda_0)N_{dd\mu}(t), \quad (11)$$

$$\frac{dN_{dt\mu}(t)}{dt} = \phi\tilde{\lambda}_{dt\mu}N^{Con.}_{\mu t}(t) - (\lambda^{f}_{dt\mu} + \lambda_0)N_{dt\mu}(t), \quad (12)$$

$$\frac{dN^{3/2}_{\mu d_{1s}}(t)}{dt} = -\lambda_0 N^{3/2}_{\mu d_{1s}}(t) - \tilde{\lambda}^{3/2}_{dd\mu}\phi N^{3/2}_{\mu d_{1s}}(t) + \frac{2}{3}\lambda_a\phi N_\mu(t) - \tilde{\lambda}^{3/2\ 1/2}_{d\mu}\phi N^{3/2}_{\mu d_{1s}}(t), \quad (13)$$

$$\frac{dN^{1/2}_{\mu d_{1s}}(t)}{dt} = -\lambda_0 N^{1/2}_{\mu d_{1s}}(t) - \tilde{\lambda}^{1/2}_{dd\mu}\phi N^{1/2}_{\mu d_{1s}}(t) + \frac{1}{3}\lambda_a\phi N_\mu(t) + \tilde{\lambda}^{3/2\ 1/2}_{d\mu}\phi N^{3/2}_{\mu d_{1s}}(t), \quad (14)$$

$$N^{Con.}_{\mu t}(t) \simeq \frac{75}{100}\frac{Y_d}{Y_0}N_{\mu p_{1s}}(t), \quad (15)$$

$$\frac{dX_c(t)}{dt} = \lambda^{f}_{dt\mu}N_{dt\mu}(t) + \lambda^{f}_{dd\mu}N_{dd\mu}(t), \quad (16)$$

for the second layer. In equation (10) the sticking of muon to tritium was neglected due to high stripping probability. The ratio Y_d/Y_0 is the probability that $t\mu$ atoms are emitted from the surface of the degrader with thickness d, where these atoms have the mean energy 2.2 eV. $Y_d(Y_0)$ is the $t\mu$-emission yield for $d \simeq 58\,\mu g\,cm^{-2}(d = 0)$ [12]. $\omega^{eff.}_s$ is the effective sticking for the cycling branch of $dt\mu$, and ω_{dd} that for the $dd\mu$ branch. $\tilde{\lambda}_{dt\mu}(s^{-1})$ is the effective formation rate for the arrangement. We define

$$\tilde{\lambda}_{dt\mu} = \tilde{\lambda}^{res.}_{dt\mu} + \tilde{\lambda}^{non.}_{dt\mu},$$

$$\tilde{\lambda}^{res.}_{dt\mu} \approx (1-\alpha)^{-1}\sum_1^3 \frac{\delta E_r}{\bar{E}_0}\lambda^{res.}_{dt\mu}(E_r)\prod_1^r P^{(r)}, \quad (17)$$

$$\tilde{\lambda}^{non.}_{dt\mu} \approx f^{non.}\lambda_{dt\mu}, \qquad f^{non.} = 1 - \sum_1^3 \frac{\delta E_r}{\bar{E}_0(1-\alpha)}\prod_1^r P^{(r)},$$

where $\prod_1^r P^{(r)}$ is the resonance escape probability. The resonance escape probability means the probability that $t\mu(1s)$ are not absorbed before falling into the energy E_r, where $P^{(1)} \simeq 1$, $P^{(2)} \simeq 0.94$ and $P^{(2)}P^{(3)} \simeq 0.67$. $(\delta E_r/\bar{E}_0(1-\alpha))\prod_1^r P^{(r)}$ approximately denotes the fractions of the μt atoms falling into the resonance energy E_r, and $f^{non.}$ the fractions of them that do not participate in the resonance. λ_0 and λ_a are the muon decay constant and the muonic atom formation rate, respectively. $\lambda^{f}_{xx\mu}(x = d, t)$ and $\lambda^{f}_{yt\mu}(y = p, d)$ are the fusion rates of the symmetric and asymmetric three body, respectively. $\tilde{\lambda}^{3/2}_{dd\mu}(\tilde{\lambda}^{1/2}_{dd\mu})$ and $\tilde{\lambda}^{3/2\ 1/2}_{d\mu}$ are the formation rate of $dd\mu^{3/2}(dd\mu^{1/2})$ and the spin-flip of $d\mu(F = 3/2)$ in solid deuterium. $\lambda_{pp\mu}$, $\lambda_{tt\mu}$, $\lambda_{dt\mu}$ and $\lambda_{pt\mu}$ are the non-resonant formation rates. The used rates and other design parameters of the two-layer arrangement are given in table 1. $\phi_0(\phi)$ is the relative number density of H/T (D_2) in units of LHD (1 LHD $= 4.25 \times 10^{22}\,cm^{-3}$). $N^{(\ )}_{(\ )}(t)$ is the evolution of the density of muon/muonic atoms or molecules in the layers (averaged density over the whole layer), where their role appears in the muon cycling coefficient X_c and also in the muon conversion efficiency.

3. Results and discussion

The muon conversion efficiency and the production of a $t\mu$ atomic beam depend on four factors. First, the muon transfer from protium to tritium competes with molecular formation $pp\mu$. Therefore, the tritium concentration must be chosen under the condition $c_t \geqslant c_p\lambda_{pp\mu}/\lambda_{pt}(\simeq 0.35 \times 10^{-3})$. Second, the thickness of the production layer must be comparable to the mean range of $t\mu$ in the same layer. Third, the H/T thickness must be larger than the distance range of the

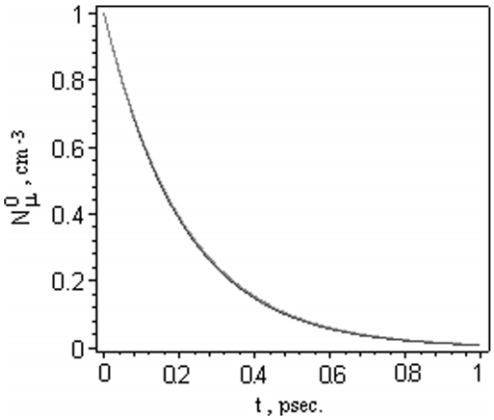

Figure 4. The muon population in the production layer $N^0_\mu(t)$ by assuming that there is no muon leakage. The shadowed region shows the error corridor for the variation parameter $\lambda_a = (3.9–4) \times 10^{12}\,s^{-1}$.

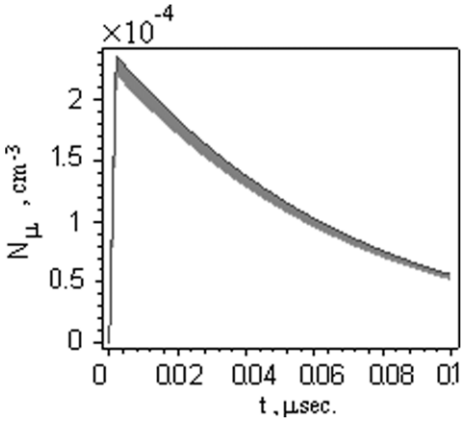

Figure 5. The muon population in the fusion layer $N_\mu(t)$ under the optimal condition. The shadowed region shows the error corridor for the variation of fractions of μp atoms transferred to tritium nuclei.

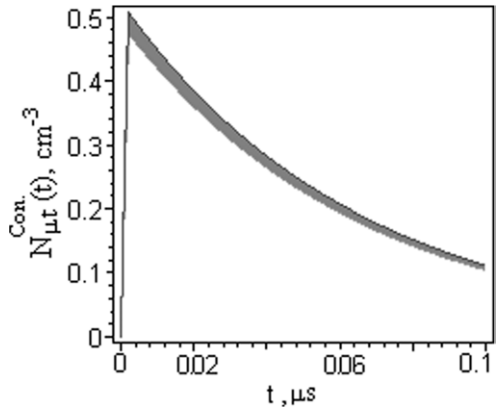

Figure 6. The population of μt emitted into the fusion layer $N^{Con.}_{t\mu}(t)$ under the optimal condition. The shadowed region shows the error corridor for the variation of fractions of μp atoms transferred to tritium nuclei.

incident muons (L_μ). Fourth, the degrader thickness must be selected under conditions where the mean energy of the muonic tritium atom becomes a little more than $E_{r=1} \simeq 1.5$ eV and also the tμ-emission yield is fairly large. With increasing thickness of the deuterium layer, large fractions of μt atoms are thermalized. To obtain such optimal conditions, the data for the production layer ($\phi_0 = 1.2$, $c_t = 10^{-3}$, $L_\mu \approx 0.4$ mm), the density $\phi = 1.43$ for D_2 and the thickness value of the degrader are extracted from recent experimental and theoretical works [1, 4, 12, 17, 18]. We have also used an accurate value of muon sticking from the literature data [19] and substituted in the rate equations. The muon sticking process is divided into two processes, initial sticking and a subsequent reactivation process, $\omega_s^{eff.} = \omega_s^0(1 - R)$, where R is the reactivation probability and ω_s^0 is the initial sticking probability. Since the initial sticking is a process immediately after a nuclear reaction, it is implied that the reactivation process depends on the temperature and density. The muon sticking $\omega_s^{eff.}$ equals ≈0.005 in the deuterium solid target kept at 3 K [19]. Assuming that there is no muon leakage from the first layer and employing the normal deuterium material at temperature 3 K, the populations $N^0_\mu(t)$, $N_\mu(t)$ and $N^{Con.}_{\mu t}(t)$ are obtained and are given in figures 4–6. The different values of X_c are presented in table 2. The muon cycling coefficient strongly depends on the population $N^{Con.}_{\mu t}(t)$, the resonance escape probability of tμ and also the resonance energy intervals. We obtain the muon conversion efficiency (ϵ_μ) as follows. ϵ_μ can be estimated simply to be the ratio of the range of the 10 keV-muon(l_μ) with respect to the range of an incident 1 MeV-muon(L_μ), multiplied by the square root of the number of μCF cycles, $(X_c)^{1/2}$. We see that the muon conversion efficiency depends on the population of slow muons in the second layer. Table 2 shows our results of the conversion efficiency. We have solved the standard equations (5)–(16), using the LSODE code.

4. Conclusions

This paper proposes a scheme which exploits the RT effect to obtain a beam of tμ atoms, which are slowed down in a layer of solid deuterium and form the dtμ molecule, which is the most important source of fusion reactions. The calculations have been performed by numerically solving the coupled equations for the population of the atomic and molecular species involved in the process. In comparison with periodical multilayers, we have found that the present two-layer arrangement is sufficient for muon cycling due to the high stopping power of slow muons. The released muons from fusion have less chance of entering into the third layer. The populations $N^0_\mu(t)$ and $N_\mu(t)$ describe this fact. The muon population in the first layer is much more than that in the fusion layer. Table 2 presents our results of the muon cycling coefficient X_c and also the muon conversion efficiency ϵ_μ under conditions that most of the μp atoms transfer to tritium nuclei. The accuracy of the results obtained in the context of the assumptions made has been shown as error corridors in figures 4–6. The same table includes the optimized values for X_c and ϵ_μ. Under the optimal condition $c_t = 10^{-3}$, $\phi_0 = 1.2$ and $\phi = 1.43$, the value of X_c equals 104.5 ± 2.5. In comparison, authors of [3] used the tritium impurity $c_t = 0.005$ (≃5 times larger than the present value) and obtained $X_c = 165$. Since large fractions of tμ atoms are absorbed before they fall down to ∼0.5 eV, the assumption of the authors of [3] (taking $\tilde{\lambda}_{dt\mu} = 0.71 \times 10^{10}$) is not correct. The numerical calculations have

Table 2. The calculated values of X_c and muon conversion efficiency ϵ_μ for the six sets ($c_t = 0.001$, $\phi_0 = 1.2$, $\phi = 1.43$), ($c_t = 0.001$, $\phi_0 = 1.46$, $\phi = 1.46$), ($c_t = 0.0012$, $\phi_0 = 1.2$, $\phi = 1.43$), ($c_t = 0.0012$, $\phi_0 = 1.46$, $\phi = 1.46$), ($c_t = 0.005$, $\phi_0 = 1.2$, $\phi = 1.43$) and ($c_t = 0.005$, $\phi_0 = 1.46$, $\phi = 1.46$).

$\tilde{\lambda}_{dt\mu}$	c_t	ϕ_0	ϕ	X_c	ϵ_μ^a
$(0.177–0.187) \times 10^{10}$	0.001	1.2	1.43	104.5 ± 2.5	0.75–0.77%
$(0.177–0.187) \times 10^{10}$	0.001	1.46	1.46	88 ± 2	0.69–0.71%
$(0.177–0.187) \times 10^{10}$	0.0012	1.2	1.43	91 ± 3	0.7–0.72%
$(0.177–0.187) \times 10^{10}$	0.0012	1.46	1.46	76.5 ± 1.5	0.65–0.66%
$(0.177–0.187) \times 10^{10}$	0.005	1.2	1.43	26.5 ± 0.5	0.38–0.4%
$(0.177–0.187) \times 10^{10}$	0.005	1.46	1.46	22.5 ± 0.5	0.35–0.36%

[a] It was experimentally estimated to be of the order of up to 1% for the arrangement H/T ⊕ D/T [6].

been performed using the LSODE computer code which the research group of [3] used. The originality of this code is presented in [20]. For the present arrangement H/T ⊕ D_2, ϵ_μ equals ∼0.7% under the optimized condition. In comparison, it has experimentally been estimated to be of the order of up to 1% for the arrangement H/T ⊕ D/T [6]. When $l_\mu(X_c)^{1/2}$ exceeds the thickness of the fusion layer, the generated muons may have a chance to be released from the surface of the fusion layer. This parameter is comparatively smaller for the arrangement of figure 2. To confirm the obtained quantities in the future, the experimental statistics must be increased, the converted muons must be measured when the set-up of figure 2 is employed. Although this set-up can be applied for the search of an efficient way of producing energy, it can be more useful in the investigation of thin materials. There are many possible applications of slow negative muons: among them the most interesting is their use in sensitive non-destructive elemental analysis. A muon stopped in matter produces x-rays when it cascades down its level ladder. These muonic x-rays are easily detectable. They provide a unique opportunity to perform elemental analysis. To study the nuclear properties, the combination of a negative slow muon beam with an ion (Z^+) beam is useful, which allows muonic atoms μZ to be formed. Among such atomic states, the atomic state which is most difficult to form is the $\mu^+\mu^-$ atom, the importance of which was emphasized by Nagamine [21]. Quantum electrodynamics (QED) can be tested without size corrections and, furthermore, because of the heavy masses of positive and negative muons, important effects, such as weak interaction correction, become highly enhanced. For more tests, both the normal and 99.7%-ortho deuterium may be applied in two separate experiments. As shown in table 2, the intensity of the slow muon beam depends on the type and density of the stopping layer. These findings may be useful for experimenters. The present results can be used in the first stage of data analysis obtained from experiments on thin surfaces of frozen hydrogen isotopes, where rough estimates are necessary to calibrate advanced models. The accuracy of the results can increase when the geometry of media is considered and the tμ-transport equation is solved. The kinetic model would be modified by the inclusion of finite media. The next stages of data analysis require more exact models based on Monte Carlo algorithms.

Acknowledgments

The author would like to thank the Persian Gulf University Research Council for financial support.

References

[1] Wozniak J. *et al* 2003 *Phys. Rev.* A **68** 062502
[2] Filipowicz M., Bystritsky V.M., Gerasimov V.V. and Wozniak J. 2008 *Eur. Phys. J.* D **47** 157
[3] Eskandari M.R. and Shirazi K. 2003 *Int. J. Mod. Phys.* C **14** 367
[4] Mulhauser F. *et al* 2006 *Phys. Rev.* A **73** 034501
[5] Ponomarev L.I. and Petitjean C. 1991 *Fusion Technol.* **20** 1022
[6] Bakule P. and Morenzoni E. 2004 *Contemp. Phys.* **45** 203
[7] Strasser P. *et al* 1996 *Hyperfine Interact.* **101/102** 539
[8] Vinnisky S.I. *et al* 1978 *Sov. Phys.—JEPT* **47** 444
[9] Gerstein S.S. and Ponomarev L.I. 1977 *Phys. Lett.* B **71** 80
[10] Vesman E.A. 1967 *Sov. Phys.—JETP Lett.* **5** 91
[11] Jones S.E. *et al* 1983 *Phys. Rev. Lett.* **51** 1757
[12] Markushin V.E. 1996 *Hyperfine Interact.* **101/102** 155
[13] Fujiwara M.C. *et al* 2000 *Phys. Rev. Lett.* **85** 1642
[14] Faifman M.P. and Ponomarev L.I. 1991 *Phys. Lett.* B **265** 201
[15] Chiccoli C., Korobov V.I., Melezhik V.S., Pasini P., Ponomarev L.I. and Wozniak J. 1992 *Muon Catalyzed Fusion* **7** 87
[16] Beckurts K.H. and Wirtz K. 1964 *Neutron Physics* (Berlin: Springer)
[17] Marshall G.M. *et al* 1999 *Hyperfine Interact.* **118** 89
[18] Toyoda A., Ishida K., Shimomura K., Nakamura S.N., Matsuda Y., Higemoto W., Matsuzaki T. and Nagamine K. 2003 *Phys. Rev. Lett.* **90** 243401
[19] Ishida K. *et al* 2001 *Hyperfine Interact.* **138** 225
[20] Hindmarsh A.C. 1983 ODEPACK, a systemized collection of ODE solvers *Scientific Computing* ed R.S. Stepleman (Amsterdam: North-Holland) pp 55–64
[21] Nagamine K. 1996 *Nucl. Phys.* B **51** 115
Nagamine K. 1983 *Proc. 3rd LAMPF II Workshop (Los Alamos, New Mexico, July 1983)* ed J.C. Allred *et al* p 258
[22] Zmeskal J., Kammel P., Scrinzi A., Breunlich W.H., Cargnelli M., Marton J., Nagele N., Werner J., Bertl W. and Petitjean C. 1990 *Phys. Rev.* A **42** 1165
[23] Petitjean C. 1992 *Nucl. Phys.* A **543** 79
[24] Hartman F.J. 1993 *Hyperfine Interact.* **82** 259
[25] Mulhauser F. *et al* 1996 *Phys. Rev.* A **53** 3069
[26] Breunlich W.H. *et al* 1987 *Muon Catalyzed Fusion* **1** 121
[27] Eliezer S. and Henis Z. 1994 *Fusion Technol.* **26** 46